Manuscript Title

Effects of vegetation change on evapotranspiration in a semiarid shrubland of the Loess Plateau, China

T. T. Gong, H. M. Lei, D. W. Yang, Y. Jiao, H. B. Yang

State Key Laboratory of Hydroscience and Engineering, Department of Hydraulic Engineering, Tsinghua University, Beijing, 100084, China

Correspondence to: H. M. Lei (leihm@tsinghua.edu.cn)

Abstract

Evapotranspiration (ET) is an important process in the hydrological cycle, and vegetation change is a primary factor that affects ET. In this study, an attempt is made to analyze the effects of vegetation change on ET using continuous observation data from eddy-covariance (EC) measurements over three periods (1 July 2011 to 30 June 2014) of a study site in a sparse shrubland study site located in the Loess Plateau of China, which is a fragile ecosystem experiencing serious soil desiccation. In our study, vegetation change includes phenological change and land use change. Phenological process of vegetation is validated to have a positive effect on normalized ET in a rate of 1.96 (the slope of normalized ET per phenological change) along with vegetation greening. Land use change at this study site is due to the removal of native vegetation by human activities, converting sparse shrubland to bare soil. With land use change during the three years, the annual amount of ET is observed to increase as well as normalized ET, suggesting that soil evaporation consumes more water than canopy

transpiration. In summary, the effects of vegetation change on ET suggest that both vegetation greening and increased area of exposed soil would aggravate the soil desiccation at the site in the north Loess Plateau.

Key words: evapotranspiration; vegetation phenology; land use change; eddy covariance; the north Loess Plateau

1 Introduction

Evapotranspiration (ET) is an important component of ecosystem water balance (Law et al., 2002; Scott et al., 2006). Previous studies have shown that more than 50% of precipitation (*P*) is consumed by ET (Yang et al., 2010; Lei, 2011), and that the ratio of ET/*P* could increase to 90% or more in semiarid and arid areas (Mo et al., 2004; Glenn et al., 2007). Therefore, a slight change in ET would have significant influences on water cycle and water resources in non-humid regions. Various factors influence ET, among which vegetation change is the most critical factor (Golchin and Asgari, 2008; Fu et al., 2004). Vegetation change mainly integrates the phenological change (temporal) and land use change (spatial). Phenological change and land use change have different mechanisms on ET rates. Phenological change controls ET rates mainly through internal physiology mainly by increasing the amount of leaf stomata with the vegetation growing and greening when the land use condition is stable (Eagleson et al., 2005), while land use change controls ET rates by converting the vegetation types which have different ET capacities (Zhang et al., 2000; Bosch and Hewlett, 1982).

The Loess Plateau is located in the upper and middle reaches of Yellow River, which is a transitional zone between the southeastern humid climate and the northwestern dry climate (Shi and Shao, 2000) with most of the precipitation falling in the summer months (Li et al., 2009). It accounts for over 40% of area of northwestern China (Zhou et al., 2005). The Loess Plateau, especially the northern part, is well-known as a region with the most severe soil erosion in the world (Cheng,

2008). Therefore, this region is ecologically fragile (Wang et al., 2011; Fu et al., 2014), in which the regional sustainable agricultural and industrial developments are seriously affected (Feng et al., 2006). The vegetation coverage is generally low, and the prevailing vegetation types are the desert shrub and desert steppe (Yang et al., 2014).

In the past few decades, vegetation condition has been observed to change substantially in this region, in terms of both phenological change and land use change (Xin et al., 2008; Jia et al., 2008; Wei et al., 2014). On one hand, a significant increasing trend of Normalized Difference Vegetation Index (NDVI) (a surrogate of vegetation phenological change) during 1981－2006 was found in the sandy land vegetation zone of north Loess region (Xin et al., 2008). Climate change with the warming temperature was considered to be a forcing factor promoting vegetation growth (Xin et al., 2008; Piao et al., 2003). On the other hand, the land use condition of this region has been constantly changing due to the human activities for the regional development (Jia et al., 2008; Gong et al., submitted). As a result, doubts about how ET will change with phenological process and different land use types have been raised.

Previous studies have assessed the impacts of vegetation change on ET by using hydrological models (Kim et al., 2005; Li et al., 2009; Cornelissen et al., 2013; Mo et al., 2004). However, model parameterization of vegetation condition is still a big challenge as it is difficult to define appropriate vegetation parameters. Therefore, the applicability and accuracy of parameters in model simulations and calibrations are

72 doubtful (Cornelissen et al., 2013). Due to the fundamental role of ET for water
73 consumption and ecosystem functioning in north China, some field experiments have
74 recently been carried out over the arid and semiarid regions of China (Zhang et al.,
75 2005; Liu et al., 2004). However, there is little learned of ET under sparsely vegetated
76 ecosystems over the north Loess Plateau, and continuous filed observations are
77 relatively poorly documented (Huang et al., 2008; Cheng et al., 2011). To bridge the
78 gap and address this issue for better understanding the role of native sparse vegetation
79 on controlling ET, this paper aims to investigate responses of ET to vegetation
80 phenological change and land use change over a period of 3 years for a sparse
81 shrubland over the north Loess Plateau.
82
83 2 Materials and methods
84 2.1 Site description
85 The study was carried out at Yulin flux site (N 38°26′, E 109°47′, 1233 m),
86 which was established in June 2011 and is in a landform transition zone changing
87 from Mu Us Sandy land to north Shaanxi Loess Plateau (Fig. 1). The study site is in a
88 semiarid continental temperate monsoon climate. According to the long-term climate
89 data (1951－2012) from a meteorological station in Yulin (Fig. 1), the annual
90 precipitation varies from 235 mm to 685 mm, with a mean of 402 mm, and more than
91 50% of annual precipitation is falling in the monsoon season (July－September). The
92 mean annual air temperature is 8.4 ℃ during the past 61 years with an annual pan
93 evaporation of 2485 mm (Wang et al., 2006). The dominant soil type is sand (98%

sand) (saturated soil water content: 0.43 m^3m^{-3}, field capacity: 0.16 m^3m^{-3}, wilting moisture content: 0.045 m^3m^{-3}) and the depth of dry sand layer is 10 cm. The mean groundwater depth of our study site during the three study years was 3.4 m.

[Figure 1 is to be inserted here]

The experimental site is covered with native xeric plants with low water demands such as *Artemisia ordosica*, a sub-shrub vegetation and *Salix psammophila*, a shrub vegetation, sparsely vegetated (Fig. 2a). They constitute the main vegetation in Mu Us Sandy Land (An et al., 2011) and are adapted well to semiarid and arid sites. According to observations around the flux tower on 14 June 2011, the maximum root depth of the native vegetation was approximately 160 cm. The vertical roots mainly (90%) distribute within 100 cm (Yang, 2012) and absorb water mainly from shallow soil of 60-80 cm (Liu et al., 2010; Yang, 2012). Xiao et al. (2005) studied that the growing season of *Artemisia ordosica* and *Salix psammophila* spanned from late April to late September. In this study, the time range from 1 May to 30 September in each year is regarded as vegetation growing season. On 15 August 2011 and 7 September 2011, surveys about vegetation coverage with randomly selected 7 samples around the flux tower (5 × 500 cm × 500 cm and 2 × 1000 cm × 1000 cm) were conducted, and it is found that the measured vegetation coverages are 28.2% and 27.9%, respectively.

[Figure 2 is to be inserted here]

At the end of June 2012, land use condition around flux tower happened to be changed by human activities. The natural native vegetation around the east area of flux tower began to be cut off (Fig. 2b), converting the land use condition from sparse

shrubland to bare soil, with the planning of replanting economical crops for grazing in the future. During the study period, the bare soil is not tilled. The area subjected to land use change was gradually becoming larger. This activity provided a unique opportunity to study the effects of land use change on ET. The study period was from 1 July 2011 to 30 June 2014, which was separated into three periods: 1 July 2011 to 30 June 2012 (2011－2012) was the first period with the initial land use condition (natural sparse vegetation); 1 July 2012 to 30 June 2013 (2012－2013) was the second period with land use condition starting to change (decreasing vegetated area and increasing area of bare soil); 1 July 2013 to 30 June 2014 (2013－2014) was the third period with largest area of land use change.

2.2 Measurements

2.2.1 EC system

Net exchange of water vapor between atmosphere and canopy at this site is measured by the eddy-covariance (EC) flux measurements, which assess the fluxes of land-atmosphere (such as water and energy) and are currently collected at a number of sites across the world as a part of FLUXNET system (Baldocchi et al., 2001). The data are essential for the estimation of the water and energy balance (Franssen et al., 2010). At this experimental site, EC system is installed at a height of 7.53 m above the ground surface, using CSAT3 three-dimensional sonic anemometers (Campbell Scientific Inc., Logan, UT, USA) for wind and temperature fluctuations, a LI-7500A open-path infrared gas analyzer (LI-COR, Inc., Lincoln, NE, USA) for water vapor,

and a CR5000 (Campbell Scientific Inc., Logan, UT, USA) data logger for data transmission.

2.2.2 Meteorological measurements

Net radiation (R_n) is measured by a net radiometer (CNR-4; KIPP&ZONEN, Delft, the Netherlands), including four radiometers measuring the incoming and reflected short-wave radiation (R_S), incoming and outgoing long-wave radiation (R_L). Wind speed and direction (05103, Young Co. Traverse City, MI, USA) are measured at 10 m above the ground surface. Precipitation (P, mm) is recorded with a tipping bucket rain gauge (TE525MM; Campbell Scientific Inc., Logan, UT, USA) installed at a height of 0.7 m above the ground surface. Air temperature (T_a) and relative humidity (R_H) are measured by a temperature and relative humidity probe (HMP45C; Campbell Scientific Inc., Logan, UT, USA) at a height of 2.6 m above the ground surface. Soil water content (θ) is measured by Time Domain Reflectometry (TDR) sensors (CS616; Campbell Scientific Inc., Logan, UT, USA), soil temperature (T_s) is measured by thermocouples (109; Campbell Scientific Inc., Logan, UT, USA), and soil heat flux (G) is measured by heat flux plates (HFP01SC; Campbell Scientific Inc., Logan, UT, USA) at a depth of 0.03 m below the ground surface. These ground variables (G, θ, T_s) are measured beneath the surface at two profiles (1) a plant canopy patch and (2) a bare soil patch. θ and T_s are measured at depths of 5, 10, 20, 40, 60, 80, 120, 160 cm below the ground surface. Groundwater table is measured by an automatic sensor (CS450-L; Campbell Scientific Inc., Logan, UT, USA), which is

160 installed in a groundwater well close to the tower.

161

162 2.3 Data and methodology

163 2.3.1 Flux data processing

164 The half-hourly latent heat flux (λET) data were calculated by EddyPro
165 (www.licor.com/eddypro), which is widely used because it is comprehensive, freely
166 available and use-friendly (Fratini et al., 2014). The available flux data sets were
167 filtered for spikes, instrument malfunctions, and poor quality, according to the
168 following criteria (Papale et al., 2006): (1) incomplete half-hourly measurements,
169 mainly caused by power failure or instrument malfunction; (2) rainy events; and (3)
170 outliers caused by occasional spikes for unknown reasons. The ratios of data removed
171 through this screening procedure are 17.3% in 2011—2012, 20.2% in 2012—2013
172 and 16.5% in 2013—2014.

173 Daily averaged flux data were calculated by firstly gap-filled half-hourly data.
174 Linear interpolation is used to fill gaps less than 1-h by calculating an average of the
175 values immediately before and after the gap. Larger gaps (gaps more than 1-h but less
176 than 7-days) in flux data are replaced by average values using mean diurnal variation
177 (MDV) methods (Falge et al. 2001). This method is adopted by FLUXNET for
178 standardized gap-filling. We found the daily mean λET had the best correlation with
179 daily mean available energy ($R_n - G$) rather than other environmental variables such
180 as vapor pressure deficit (VPD) and NDVI. Therefore, for some large gaps more than
181 7-days in daily mean λET, we simulated the relationship between daily mean λET (y)

and daily mean available energy flux ($x = R_n - G$) in each period ($y = f(x)$). Then we used the simulated function f to estimate daily mean λET of gaps. We chose the function f with the highest coefficient of determination (R^2) in each period (Yan et al., 2013). The function f of each period are $y = 0.0014\,x^2 + 0.0746\,x + 10.69$ (R^2 = 0.60), $y = 0.0012x^2 + 0.0559x + 17.69$ (R^2 = 0.45), and $y = 0.0014x^2 + 0.16x + 13.244$ (R^2 = 0.56), respectively. Large gaps of more than 7-days did occur in the winter.

2.3.2 Footprint model

In order to determine the contributing source area of flux at our study site, scalar flux footprint model was used. Heish et al. (2000) has proposed an analytic model that accurately described the relationship between footprint, observation height, surface roughness, and atmospheric stability. The footprint fetch F_f was calculated from (Heish et al, 2000),

$$\mathrm{F_f/Z_m} = \mathrm{D}/(0.105 \times \mathrm{k^2})\,\mathrm{Z_m^{-1}|L|^{1-Q}Z_u^{Q}} \quad (1)$$

where k is the von Karman constant (0.40), D and Q are the similarity constants (stable conditions: D = 0.28, Q = 0.59; near neutral and neutral conditions: D = 0.97, Q = 1; unstable conditions: D = 2.44, Q = 1.33), L is the Obukhov Length, Z_m is the height of instrument, and it is in a range of 2 to 20 m, Z_u is defined as (Heish et al, 2000),

$$\mathrm{Z_u} = \mathrm{Z_m}(\ln(\mathrm{Z_m/Z_{0m}}) - 1 + \mathrm{Z_m/Z_{0m}}) \quad (2)$$

where Z_{0m} is the height of momentum roughness, and it ranges from 0.01 to 0.1 m.

204

205 2.3.3 Methods of analyzing the control of vegetation change on ET

206 It is generally recognized that potential evapotranspiration (E_{TP}), vegetation
207 condition and soil water content are the three main parameters controlling ET
208 (Lettenmaier and Famiglietti, 2006; Chen et al., 2014). In order to decouple the effect
209 of vegetation change from the integrated effects of these three factors on ET, we used
210 a simple equation which is similar with the FAO single crop coefficient method
211 (Irrigation and Drainage Paper No. 56 (FAO-56)) and is expressed as,

212 $$\mathrm{ET} = \mathrm{E_{TP}} \times f_v(\text{vegetation}) \times f_s(\text{soil water}) \quad (3)$$

213 where $f_v(\text{vegetation})$ represents the effect of vegetation change on ET, and
214 $f_s(\text{soil water})$ represents the effect of soil water content on ET. By transforming the
215 Eq.3, $f_v(\text{vegetation})$ can be expressed as,

216 $$f_v(\text{vegetation}) = \mathrm{E_T}/[\mathrm{E_{TP}} \times f_s(\text{soil water})] \quad (4)$$

217 where $f_v(\text{vegetation})$ can also be regarded as the normalized ET which eliminates
218 the effects of atmospheric and soil water content. E_{TP} (mm day^{-1}) was estimated by
219 the following equation (Maidment, 1992) which is a modification of Penman
220 equation,

221 $$\mathrm{E_{TP}} = \frac{\Delta}{\Delta+\gamma}(\mathrm{R_n} - \mathrm{G}) + \frac{\rho_a c_p / r_a}{\Delta+\gamma}\frac{\mathrm{VPD}}{\lambda} \quad (5)$$

222 where the units of Rn and G are mm d^{-1}; ρ_a is the air density ($= 3.486\frac{P}{275+T}$, kg m^{-3},
223 where P is the atmospheric pressure in kPa and T is air temperature in degrees
224 Celsius); c_p is the specific heat of moist air (=1.013 kJ kg^{-1} ℃$^{-1}$); Δ is the slope of
225 saturation vapor-pressure-temperature curve (kPa ℃$^{-1}$); γ is the psychrometric

constant (kPa ℃$^{-1}$); U_2 is the daily mean wind speed at a height of 2.0 m (m s^{-1}); VPD is the difference of the mean saturation vapor pressure (e_s, kPa) and actual vapor pressure (e_a, kPa); r_a is the aerodynamic resistance, which was calculated as (Penman, 1948; 1963),

$$r_a(\mathrm{s/m}) = \frac{4.72[ln(\frac{Z_h}{Z_0})][ln(\frac{Z_h}{Z_0})]}{1+0.536U_2} \quad (6)$$

where Z_h is the height at which meteorological variables are measured (2 m), and Z_0 is the aerodynamic roughness of surface (0.00137 m) (Penman, 1948; 1963).

The effects of soil water content on ET can be described in three stages (Idso et al., 1974), stage 1: the soil water is enough to satisfy the potential evaporation rate (f_s=1); stage 2: the soil is drying and water availability limits ET (0<f_s<1); and stage 3: the soil is dry and it can be considered negligible (f_s=0). Therefore, we used daily mean soil water content of the root depth (θ_r) and soil surface (θ_s) to estimate f_s by the following expression (Hu et al., 2006),

$$f_s = \begin{cases} = 1 & \theta > \theta_k \\ = 0 & \theta < \theta_w \\ = \frac{\theta-\theta_w}{\theta_k-\theta_w} & \theta_w \le \theta \le \theta_k \end{cases} \quad (7)$$

where θ_w is the wilting value, θ_k is the stable field capacity which is considered to be equivalent to 60% of the field capacity (Lei et al., 1988; Wang et al., 2008). In this study, f_{sr} and f_{ss} were defined as the effects of soil water content of root zone and surface on ET, respectively, and they were calculated as,

$$f_{sr} = \frac{\theta_r-\theta_w}{\theta_k-\theta_w} \quad (\theta_w \le \theta_r \le \theta_k) \quad (8)$$

$$f_{ss} = \frac{\theta_s-\theta_w}{\theta_k-\theta_w} \quad (\theta_w \le \theta_s \le \theta_k) \quad (9)$$

where θ_r and θ_s were calculated by actual measured soil water contents at different

depths, θ_r ($m^3\,m^{-3}$) is the mean soil water content from surface to the depth of 160 cm (root zone), and was calculated as,

$$\theta_r = \frac{0.5[10\theta_5+15\theta_{10}+30\theta_{20}+40(\theta_{40}+\theta_{60})+60\theta_{80}+80\theta_{120}+40\theta_{160}]}{160} \quad (10)$$

θ_s ($m^3\,m^{-3}$) is the mean surface soil water content (0—10cm), and was calculated as (Moran et al., 2009),

$$\theta_s = \frac{\theta_5+\theta_{10}}{2} \quad (11)$$

Site-averaged soil water content of each depth ($\theta_i; i$ =5, 10, 20, 40, 60, 80, 120, and 160) was calculated at each depth by taking the weighted mean values of the canopy and bare surface measurements by the percent coverage,

$$\theta_i = M \times \theta_{i,c} + (1 - M) \times \theta_{i,b} \quad (12)$$

where $\theta_{i,c}$ and $\theta_{i,b}$ refer to the measured soil water content of canopy patch and bare soil patch at the depth of i cm (some results of past researchers have figured out that if only one single soil water content ($\theta_{i,c}$ or $\theta_{i,b}$) was used, it would yield an error of roughly 25% (Kustas et al., 2000)); M is the monthly mean vegetation coverage, and it was calculated by monthly mean NDVI values (Gutman and Ignatov, 1998),

$$M = (NDVI - NDVI_{min})/(NDVI_{max} - NDVI_{min}) \quad (13)$$

where $NDVI_{max}$ is the maximum value (0.8 in this study); $NDVI_{min}$ is the minimum value (0.05 in this study) (Gutman and Ignatov, 1998); NDVI is daily mean value that calculated by the following Eq.15. The calculated monthly *M* was validated according to the actual measured vegetation coverage in our study site.

Vegetation change includes vegetation phenological change and land use type

change. In this study, vegetation phenology is represented by Moderate Resolution Imaging Spectroradiometer (MODIS)-NDVI data when land use condition is stable. The MODIS-NDVI is sufficiently stable to reflect the seasonal changes of any vegetation (Huete et.al, 2002), and the daily MODIS/Terra and MODIS/Aqua Surface Reflectance (at 250m) data within the footprint source area were chosen. The Surface Reflectance data of MODIS/Terra (MOD09GQ) and MODIS/Aqua (MYD09GQ) are downloaded from reverb (http://reverb.echo.nasa.gov) for the period from 1 July 2011 to 30 June 2014. MODIS Reprojection Tool (MRT) (Kalvelage and Willems, 2005) was used to reject the daily Surface Reflectance data to the Universal Transverse Mercator (UTM). MODIS surface reflectance bands 1 and 2 (at 250m) were used to calculate NDVI,

$$\mathrm{NDVI}_{Terra\ or\ Aqua} = \frac{\mathrm{bands2}-\mathrm{bands1}}{\mathrm{bands2}+\mathrm{bands1}} \quad (14)$$

In order to eliminate the poor quality data values caused by rain and cloud events, the estimated NDVI data stack needs to be firstly filtered to remove anomalous hikes and drops (Lunetta et al., 2006). Hikes and drops were eliminated by removing the values that suddenly decreased or increased, and then smoothing spline was used to produce a smoother profile. In this study, daily mean NDVI was calculated as,

$$NDVI = \frac{NDVI_{Terra}+NDVI_{Aqua}}{2} \quad (15)$$

Theoretically, land use change can be evaluated by comparing the land use maps in two different periods. However, the transient land use maps are unavailable at our study site. Therefore, in this study, we introduced an indicator of D_{lu} to be the measure of land use change. We separated the study area into two zones. We assigned

291 the zone without land use change as zone A, and assigned the zone with land use
292 change as zone B. In zone A, there was mainly the vegetation phenological change
293 during the three years; however, in zone B, there were not only vegetation
294 phenological change but also land use change. Therefore, land use change can be
295 calculated by the following equation,

296 $$D_{lu} = M_A - M_B \quad (16)$$

297 where M_A and M_B are the vegetation coverage of zone A and zone B, respectively.
298 D_{lu} reflects land use change most exactly in summer than in winter, because M is a
299 measure of the fraction of green vegetation and D_{lu} in winter is meaningless and
300 nearly zero. Therefore, we selected the mean D_{lu} of July—September in each period
301 to analyze the impacts of land use change on ET.

302

303 # 3 Results

304 ## 3.1 Footprint and energy balance closure

305 Based on the footprint model, we got the half-hourly scatter data of footprint
306 fetch (Eq. (1)). According to the wind rose (Fig. 3a), the main and strong wind
307 directions in this site are northwest and southeast, so we chose an ellipse to enclose
308 the scatters and simulated the footprint (Fig. 3b). The footprint was validated as there
309 were 93% half-hourly flux data within the ellipse under unstable conditions.

310 [Figure 3 is to be inserted here]

311 We measured the boundary of zone B until October 2013 when the land use
312 condition in zone B had stopped to change (Fig.3b). There were 11 pixels (250 m ×

250 m) in zone A and 19 pixels (250 m × 250 m) in zone B, and thus in the following parts of calculating the weight-averaged NDVI ($NDVI_w$) within footprint, we chose the weighted coefficient as $\beta = 11/(11 + 19)$.

In order to validate EC measurements and examine the quality of flux data, we used daily mean flux data of 2011—2012 to conduct the linear regression between available energy ($R_n - G$) and the sum of surface fluxes ($\lambda ET + H$). The linear regression yielded a slope ~ (0.87), an intercept of -1.42 W m^{-2} and R^2 of 0.82. These indicators indicated that the measurements at our experimental site provided reliable flux data, and that the EC measurements underestimated the sum of surface fluxes to the extent of 13%. A lot of studies have investigated the energy imbalance (Barr et al., 2006; Wilson et al., 2002; Franssen et al., 2010), and there is a consensus that it is difficult to examine the exact reasons leading to the imbalance.

3.2 Characteristics of environmental variables

A brief summary of the key environmental variables is presented in this section. The seasonal and inter-annual characteristics of monthly mean T_a, R_H, sunshine duration (D_S), P (Fig. 4) , and daily mean NDVI (Fig. 5(a, b)) were analyzed.

[Figure 4 is to be inserted here]

Monthly mean T_a during the three study periods were around the climatological normal (1954—2012), sharing higher values in summer (June—August) and lower values in winter (December—February of the next year). Annual mean T_a of 2012—2013 and 2013—2014 were 8.5 °C and 8.9 °C, respectively, which were both a little

335 higher than the normal (8.4 °C), and annual mean T_a of 2011－2012 was 7.6 °C,
336 which was a little lower than 8.4 °C. Mean T_a in monsoon season of each study
337 period were 19.0 °C, 19.2 °C and 19.7 °C, respectively, which were all slightly lower
338 than the normal (20.2 °C). Higher R_H occurred in August and lower R_H was in April.
339 Annual mean R_H of 2011－2012 was 56.9%, which was above the normal (55.3%).
340 However, annual mean R_H in 2012－2013 and 2013－2014 were 48.0% and 49.3%,
341 respectively, and they were both lower than 55.3%. Mean R_H of monsoon season were
342 65.3% in 2011－2012, 64.4% in 2012－2013, 65.5% in 2013－2014, and they were
343 all nearly the same as the normal (65.3%). Seasonal D_S had the same trend with T_a.
344 Daily mean D_S of monsoon season in each period were basically the same (8.1 h in
345 2011－2012, 8.5 h in 2012－2013, and 8.2 h in 2013－2014), and they were all above
346 the normal (8.0 h). There were 94 rainy days in 2011－2012 (total P: 486.8 mm), 75
347 rainy days in 2012－2013 (total P: 484 mm), and 72 rainy days in 2013－2014 (total
348 P: 453.3 mm).

349 [Figure 5 is to be inserted here]

350 Seasonal NDVI curve with stable land use condition (in zone A or in zone B
351 during the period of 2011-2012) represented the process of vegetation phenology and
352 it had a single peak value in each year (Fig. 5). In early May, seasonal NDVI curve
353 began to increase and native vegetation began to enter the growing season and
354 reached to the maximum value (0.27±0.01) in July or August. In winter, daily mean
355 NDVI stayed at a nearly constant value (0.12). For zone A (Fig. 5a), the peak values
356 during the three years were nearly the same (0.26~0.27). While for zone B (Fig. 5b),

the peak values declined year by year (0.28, 0.25, and 0.15) due to the removal of native vegetation by human activities. In the second period, the land use condition in zone B was the mixture of natural vegetation and bare soil, so the maximum NDVI of this period was a little lower than the first period. As time went on, some places in zone B that encountered the land use change earlier had come up with some ruderal, which contributed to the consequence that the maximum NDVI value of the third single-peak curve was slightly more than NDVI value of bare soil.

[Figure 6 is to be inserted here]

The results of D_{lu} in each period were shown in Fig.6. Due to the tiny differences in spatial distributions of natural vegetation, D_{lu} of the first period was negative. Compared to the first period (2011-2012) with natural land use condition, D_{lu} of 2012-2013 and 2013-2014 increased. Taking August in each period as an example, in August of 2011-2012, D_{lu} was -1.5%, while in August of 2012-2013 and 2013-2014, D_{lu} were 2.4% and 13.1%, respectively.

3.3 Phenological change controls on ET

Seasonal curve of ET in each year had a single peak value (Fig.7a), and the higher ET appeared mostly in summer while the lower appeared in winter. The mean ET in summer of the whole three periods was 1.9 mm day^{-1}, and in winter, it was 0.4 mm day^{-1}. The daily mean ET was in a range from 0.002 mm day^{-1} to 5.8 mm day^{-1} during the three periods with the highest daily mean ET on 30 June 2014, which was the day after a rainfall event of 14.8 mm. ET increases after rainfall events, because after rainy days, evaporation is much higher and accounts for most of

evapotranspiration. The lowest ET was on 28 November 2012, which was in the frozen period (late November to early March in our study site).

[Figure 7 is to be inserted here]

The $NDVI_w$ (Fig. 7c) was estimated by $NDVI_w = NDVI_A \times \beta + NDVI_B \times (1 - \beta)$, where $NDVI_A$ and $NDVI_B$ were daily mean NDVI values of zone A and zone B; β was the weighted coefficient ($\beta = 11/30$). $NDVI_w$ (Fig.7c) had one peak value in each year as well as the curves of $NDVI_A$ and $NDVI_B$. However, E_{TP} (Fig.7b) had two peak values in summer of 2013, while only one peak value appeared in 2012. During the three periods, E_{TP} was in the range from 0.16 mm day^{-1} in winter to 18 mm day^{-1} in summer. f_{ss} and f_{sr} (Fig. 7d) increased rapidly in response to heavy and weak rainfall events of more than 5 mm a day, and also decreased rapidly one or two days later after rainfall events, especially f_{ss}. During late November to early March, there was a frozen period of this site, and soil water content was below the wilting point, thus in this period, f_{ss} and f_{sr} were both very small. The mean values of E_{TP}, $NDVI_w$, f_{ss} and f_{sr} in summer of the whole three years were 7 mm, 0.22, 0.62, and 0.60, respectively, while in winter, they were 2 mm, 0.13, 0.03, and 0.12, respectively.

In order to investigate the major seasonal factor that controls ET at our study site, the correlations between ET and the three factors (E_{TP}, $NDVI_w$, f_s (f_{ss} and f_{sr})) were analyzed and shown in Fig. 8(a, b, c, d) based on daily mean data in 2011—2012. The reason we chose the data of 2011-2012 was that the seasonal $NDVI_w$ curve reflected the phenological change of natural vegetation. Data in rainy days and frozen days were removed, because in rainy days, ET was gap-filled instead of actual

402 measured. In frozen days, native vegetation was withered with no transpiration and
403 soil water was in frozen status with little evaporation. Partial correlations and
404 significant T-test were calculated to evaluate the degree of correlation.

405 [Figure 8 is to be inserted here]

406 The partial correlation coefficients (PCC) between ET and $NDVI_w$ (PCC=0.72),
407 E_{TP} (PCC=0.61) are both larger than 0.355 ($r_{0.05}$), indicating that ET has an obvious
408 linear relationship with $NDVI_w$ ($p<0.05$) and E_{TP} ($p<0.05$). PCC between ET and f_{ss}
409 (0.23) is much better than f_{sr} (0.06). The linear correlations between ET and $NDVI_w$
410 (Fig.8a), E_{TP} (Fig.8b) both pass the 95% t-test confidence level, while the significant
411 t values of linear relations between ET and f_{ss}, f_{sr} are both not significant at the 95%
412 level, R^2 are also very small ($R^2 < 0.1$).

413 To better quantify the effects of phenological process on ET, daily mean ET and
414 $NDVI_w$ in 2011—2012 were analyzed (Fig.9). Guo et al. (2000) have found that in
415 Mu Us Sandy Land, the water would not infiltrate fully into the root zone of shrub
416 vegetation and would be mainly consumed as evaporation (E) from surface soil after
417 the total rain less than 25 mm. In order to accurately describe the controlling degree of
418 vegetation phenological change on ET, we removed the daily data that when
419 antecedent rainfall was less than 25 mm.

420 [Figure 9 is to be inserted here]

421 Linear regressions are found between f_{vr} ($f_{vr} = ET/(E_{TP} \times f_{sr})$) and $NDVI_w$
422 (Fig.9a), and the same as between f_{vs} ($f_{vs} = ET/(E_{TP} \times f_{ss})$) and $NDVI_w$ (Fig.9b).
423 The slopes of linear regressions were used to evaluate the controlling degree between

ET and vegetation phenological process. The ratio of $f_{vs}/\mathrm{NDVI_w}$ is 1.95, approximately equals to $f_{vr}/\mathrm{NDVI_w}$ (1.97). The regression between f_{vr} and $\mathrm{NDVI_w}$ has somewhat more scatter (R^2 = 0.57) than the equivalent regression between f_{vs} and $\mathrm{NDVI_w}$ ($R^2 = 0.66$). The two regressions state the direct positive relationship between $\mathrm{NDVI_w}$ and normalized ET, indicating that when $\mathrm{NDVI_w}$ increases one unit, it will contribute normalized ET to increase about 1.96 units. R^2 of the two linear normalized regressions are both higher than R^2 of un-normalized regression ($R^2 = 0.50$), and the increase in normalized ET is obviously associated with landscape $\mathrm{NDVI_w}$.

3.4 Land use change controls on ET

The mean daily ET were 1.02 mm day^{-1} in 2011—2012, 1.14 mm day^{-1} in 2012—2013, and 1.33 mm day^{-1} in 2013—2014. The daily mean ET of growing season in 2011—2012 were 1.7 mm day^{-1}, 1.8mm day^{-1} in 2012—2013, and 2.1 mm day^{-1} in 2013—2014. Mean f_s in each year were basically at the same level (f_{ss}: 0.49±0.02; f_{sr}: 0.45±0.01), and the same as in the growing season of each year. Compared to 2011—2012 (4.3 mm day^{-1}), daily mean E_{TP} in 2012—2013 increased 1.0 mm day^{-1}, and it increased 0.9 mm day^{-1} in 2013—2014.

[Figure 10 is to be inserted here]

Quantitative results of the relationship between D_{lu} and normalized ET (f_{vr} and f_{vs}) are shown in Fig. 10. Compared to 2011—2012, f_{vr} and f_{vs} of July—September in 2012—2013 increased by 3.1 and 3.0, while in 2013—2014, f_{vr} and

446 f_{vs} increased by 10.8 and 9.4. According to the linear regressions, if E_{TP} keeps stable
447 and D_{lu} increases 1%, normalized ET at our experimental site will increase 0.8~0.9
448 mm.
449
450 4 Discussion
451 4.1 Implications of the impacts of phenological change on ET
452 The correlations between ET and its controlling factors indicate that at our
453 experimental site, E_{TP} and $NDVI_w$ are the primary factors affecting the seasonal ET.
454 However, f_s, especially f_{sr}, has no significant effect on ET. In our study, the
455 relationship between normalized ET and daily $NDVI_w$ (Fig.9) in 2011-2012 indicates
456 that at our study site, when land use condition is stable, seasonal ET is mainly
457 determined indirectly by the amount of greenness at the seasonal scale, rather than
458 water supply from soil moisture directly. This result further implies that vegetation
459 acts as a buffer of dramatic soil moisture variability in this semiarid region. During a
460 year with stable land use condition, when vegetation turns green, the numbers of leaf
461 stomata will increase and more water will be transpired from leaves to atmosphere.
462 Various studies have tested the relationships between phenological change and ET,
463 and these results generally showed consistent and positive linear relationships. In
464 different vegetation ecosystems, phenological change is reported to affect ET in
465 different degrees (Xu et al., 2008). For example, strong linear regression between
466 phenological change and ET was found in several forests and non-irrigated cropland
467 (slopes of linear regressions > 30) (Running et al., 1988; Loukas et al., 2005). Kondoh
468 et al. (1995) have demonstrated that phenological change had a strong influence on

ET in a dense grassland at Kendall, Arizona (slope of the linear regression = 14.2). For high dense vegetated ecosystems such as forests and grasslands, phenological change has a strong and significant control on ET. However, in low vegetated ecosystems such as sparse shrubland, the relationship between ET and phenological change is thus positive but relative weak.

The positive effect of phenological change on normalized ET indicates that under stable land use condition, if E_{TP} keeps stable and vegetation is greening (Xin et al., 2008), normalized ET rates will increase. This increase of normalized ET will consume more water and result in aggravating the water deficiency of north Loess Plateau, contributing to the formation of more dried soil and more severe soil desiccation in the future.

4.2 Effects of land use change on ET

The quantitative analysis (Fig.6, Fig.10, Table 1) showed that when the mean D_{lu} during the three periods changed from -1.0% to 11.5%, f_{vr} increased from 28.1 to 38.9 (f_{vs}: 27.7-37.1), indicating that at our experimental site, land use condition converted from native sparsely distributed vegetation to bare soil led to an increase in normalized ET. The possible reason for this increase of normalized ET is that the normalized soil evaporation from each unit was larger than transpiration from each unit. Our results implies that in sparse shrublands, soil evaporation (E) might take larger portion than transpiration (T). This result is consistent with other findings in sparsely vegetated ecosystems (Kurc and Small, 2004; Zhang et al., 2005; Mu et al.,

2007; Holm et al., 2003; Huxman et al., 2005), but is opposite with the findings in high dense vegetated ecosystems such as forests where *T* is reported to take greater proportion than *E* (Huang et al., 2010; Hu et al., 2013; Wang and Yakir, 2000).

The north Loess Plateau is a low dense vegetated region and becoming fragile (Liang et al., 2008). Our result that land degradation can increase the normalized ET implies that the soil desiccation may aggravate with land degrading in the north Loess region. Accompanied by land degradation, more area of bare soil has been exposed, which would also increase soil erosion in the exposed area and contribute to further degradation of the north Loess region (Ludwig et al., 2005).Therefore, optimizing land use structure of the north Loess Plateau may promote the sustainable environmental development by effectively controlling soil desiccation.

5 Conclusion

In this study, based on the continuous observation data from eddy-covariance (EC) measurements over three periods (1 July 2011 to 30 June 2014), we found that the daily mean ET was in a range from 0.002 mm day^{-1} to 5.8 mm day^{-1} and the annual amount ET were 375 mm in 2011-2012, 417 mm in 2012-2013, and 478 mm in 2013-2014. Impacts of vegetation change (vegetation phenological change and land use change) on ET were analyzed, and normalization method was used to exclude the effects of meteorological condition and soil water condition on ET. Our results showed that vegetation phenological change had a positive effect on seasonal variations of ET, and normalized ET increased at a rate of 1.96 (the slope of

513 normalized ET per $NDVI_w$) with the vegetation greening. Also, land use change
514 (sparse vegetation was converted to bare soil) enhanced ET, normalized ET was
515 observed to increase from 28.1 in 2011-2012 to 38.9 in 2013-2014. And this increase
516 of normalized ET is due to the more amount of increased soil evaporation than the
517 amount of decreased transpiration. Our study suggested that both vegetation greening
518 and land degradation might accelerate ET rates and aggravate the soil desiccation in
519 the north Loess Plateau.
520
521 **Acknowledgements**

522 This research was supported by the National Natural Science Foundation of China
523 (Project Nos. 51209117 and 51139002), the Basic Research Fund Program of State
524 key Laboratory of Hydroscience and Engineering (Grant No. 2014-KY-04) and the
525 Hydraulic Science and Technology Plan Foundation of Shaanxi Province
526 (2013slkj-08). We thank A. W. Jayawardena for language and constructive
527 suggestions of the manuscript.
528
529 **References**

530 An, H. and An, Y.: Soil moisture dynamics and water balance of Salix psammophila shrubs in south
531 edge of Mu Us Sandy Land]. Journal of applied ecology 22, 2247-2252,2011
532 Baldocchi, D. D. and Wilson K. B.: Modeling CO_2 and water vapor exchange of a temperate
533 broadleaved forest across hourly to decadal time scales, Ecological Modelling, 142, 155-184, 2001.
534 Barr, A. G., Morgenstern, K., Black, T. A., McCaughey, J. H.and Nesic, Z.: Surface energy balance

535 closure by the eddy-covariance method above three boreal forest stands and implications for the
536 measurement of the CO2 flux. Agricultural and Forest Meteorology, 140, 322-337, 2006.
537 Chen, Y., Xia, J. Z., Liang, S. L., Feng, J. M., Fisher, J. B., Li, X., Li, X. L., Liu, S. G., Ma, Z. G.,
538 Miyata, A., Mu, Q. Z., Sun, L., Tang, J. W., Wang, K. C., Wen, J., Xue, Y. J., Yu, G. R., Zha, T. G.,
539 Zhang, L., Zhang, Q., Zhao, T. B., Zhao, L. and Yuan, W. P.. Comparison of satellite-based
540 evapotranspiration models over terrestrial ecosystems in China. Remote Sensing of Environment, 140,
541 279-293, 2014.
542 Cheng, X. R.: Water transformation and simulation of soil-artificial vegetation-atmosphere-transfer in
543 the farming-pastoral zone of the Loess Plateau, Graduate University of Chinese Academy of Sciences,
544 Shaanxi, Phd thesis, 2008 (in Chinese)
545 Cheng, X. R., Yu, M. K., Huang, M. B. and Shao, M. A.: Simulation of energy balance of SVAT
546 system in the farming-pastoral zone of the Loess Plateau, Acta prataculturae sinica, 20, 160-168, 2011,
547 (in Chinese)
548 Cornelissen, T., Diekkrüger, B. and Giertz, S.: A comparison of hydrological models for assessing the
549 impact of land use and climate change on discharge in a tropical catchment, Journal of Hydrology, 498,
550 221-236, 2013.
551 Eagleson, P. S.. Ecohydrology: Darwinian expression of vegetation form and function. Cambridge
552 University Press, 2005.
553 Fan, X. G., Ma, Z. G., Yang, Q., Han, Y. H., Mahmood, R.: Land use/land cover changes and regional
554 climate over the Loess Plateau during 2001-2009.Part Ⅱ： interrelationship from observations. Climate
555 Change, doi 10.1007/s10584-014-1068-5/, 2014
556 Falge, E., Baldocchi, D., Olson, R., Anthoni, P., Aubinet, M., Bernhofer, C., Burba, G., Ceulemans, R.,

557 Clement, R., Dolman, H., Granier, A., Gross, P., Grunwald, T., Hollinger, D., Jensen, N. O., Katul, G.,
558 Keronen, P., Kowalski, A., Lai, C. T., Law, B. E., Meyers, T., Moncrieff, H., Moors, E., Munger, J. W.,
559 Pilegaard, K., Rannik, U., Rebmann, C., Suyker, A., Tenhunen, J., Tu, K., Verma, S., Vesala, T.,
560 Wilson, K. and Wofsy, S.: Gap filling strategies for long term energy flux data sets. Agricultural and
561 Forest Meteorology, 107, 71-77, 2001.
562 Feng, J., Wang, T. and Xie, C.: Eco-environmental degradation in the source region of the Yellow
563 River, Northeast Qinghai-Xizang Plateau, Environmental monitoring and assessment, 122, 125-143,
564 2006.
565 Fratini, G. and Mauder, M.: Towards a consistent eddy-covariance processing: an intercomparison of
566 EddyPro and TK3, Atmospheric measurement techniques, 7, 2273-2281, 2014.
567 Franssen, H. J., Stoeckli, R., Lehner, I., Rotenberg, E. and Seneviratne, S. I.: Energy balance closure of
568 eddy-covariance data: A multisite analysis for European FLUXNET stations. Agricultural and forest
569 meteorology, 150, 1553-1567, 2010.
570 Fu, B. J., Liu, S. L., Chen, L. D., Lu, Y. H. and Qiu, J.: Soil quality regime in relation to land cover and
571 slope position across a highly modified slope landscape. Ecological Research, 19, 111-118, 2004.
572 Fu, Q., Lu, L.and Huang, J.: Numerical Analysis of Surface Runoff for the Liudaogou Drainage Basin
573 in the North Loess Plateau, China, Water Resources Management, 1-14, 2014.
574 Glenn, E. P., Huete, A. R., Nagler, P. L., Hirschboeck, K. K. and Brown, P.: Integrating remote sensing
575 and ground methods to estimate evapotranspiration, Critical Reviews in Plant Sciences, 26, 139-168,
576 2007.
577 Golchin, A. and Asgari, H.: Land use effects on soil quality indicators in north-eastern Iran, Soil
578 Research, 46, 27-36, 2008.

579 Guo, K., Dong, X. J. and Liu, Z. M.: Characteristics of soil moisture content on sand dunes in mu us
580 sandy grassland: why *artemisia ordosica* declines on old fixed sand dunes, Acta phytoecologica sinica,
581 24, 243-247, 2000 (in Chinese)
582 Gutman, G. and Ignatov, A.: The derivation of the green vegetation fraction from NOAA/AVHRR data
583 for use in numerical weather prediction models, International Journal of Remote Sensing, 19,
584 1533-1543, 1998.
585 Holm, A. M., Cridland S. W. and Roderick, M. L.: The use of time-integrated NOAA NDVI data and
586 rainfall to assess landscape degradation in the arid shrubland of Western Australia, Remote Sensing of
587 Environment, 85, 145-158, 2003.
588 Heish, C. I., Katul G. and Chi, T. W.: An approximate analytical model for footprint estimation of
589 scalar fluxes in thermally stratified atmospheric flows. Advances in Water Resources, 23, 765-772,
590 2000.
591 Hu, H. H., Dai, M. Q., Yao, J. L., Xiao, B. Z., Li, X. H., Zhang, Q. F. and Xiong, L. Z.: Overexpressing
592 a NAM, ATAF, and CUC (NAC) transcription factor enhances drought resistance and salt tolerance in
593 rice, Proceedings of the National Academy of Sciences, 103, 12987-12992, 2006.
594 Huang, J., Zhang, W., Zuo, J. Q., Bi, J. R., Shi, J. S., Wang, X., Chang, Z. L., Huang, Z. W., Yang, S.,
595 Zhang, B. D., Wang, G. Y., Feng, G. H., Yuan, J. Y., Zhang, L., Zuo, H. C., Wang,S. G., Fu, C. B.,
596 Chou, J. F.: An overview of the semi-arid climate and environment research observatory over the Loess
597 Plateau. Advances in atmospheric sciences, 25, 906-921, 2008.
598 Huete, A., Didan, K., Miura, T., Rodriguez, E. P., Gao, X. and Ferreira, L. G.: Overview of the
599 radiometric and biophysical performance of the MODIS vegetation indices. Remote sensing of
600 environment, 83, 195-213, 2002.

601 Huxman, T.E., Wilcox, B. P., Breshears, D. D., Scott, R. L., Snyder, K. A., Small, E. E., Hultine, K.,
602 Pockman, W. T., Jackson, R. B.: Ecohydrological implications of woody plant encroachment, Ecology,
603 86, 308-319, 2005.
604 Idso, S.B., Reginato, R. J., Jackson, R. D., Kimball, B. A. and Nakayama, F. S.: The three stages of
605 drying of a field soil, Soil Science Society of America Journal, 38, 831-837, 1974.
606 Jia, K. L., Chang, Q. R., Zhang, J. H.: Analysis of land use changes and driving mechanisims in the
607 mixed agriculture-livestock production region in northern Shaanxi. Resources science, 30, 2008 (in
608 Chinese)
609 Kalvelage, T., Willems, J.: Supporting users through integrated retrieval, processing, and distribution
610 systems at the Land Processes Distributed Active Archive Center, Acta astronautica, 56, 681-687,
611 2005.
612 Kim, W., Kanae, S., Agata, Y., Oki, T.: Simulation of potential impacts of land use/cover changes on
613 surface water fluxes in the Chaophraya river basin, Thailand, Journal of Geophysical Research:
614 Atmospheres (1984-2012), 110, 2005.
615 Kondoh, A.: Changes in evapotranspiration due to anthropogenic changes in land cover in monsoon
616 Asia. J. Jpn. Soc. Photogrammetry and remote Sensing, 34, 13-21, 1995.
617 Kurc, S. A. and Small, E. E.: Dynamics of evapotranspiration in semiarid grassland and shrubland
618 ecosystems during the summer monsoon season, central New Mexico, Water Resources Research, 40,
619 2004. doi:10.1029/2004WR003068
620 Kustas, W. P. and Norman, J. M.: A two-source energy balance approach using directional radiometric
621 temperature observations for sparse canopy covered surfaces, Agronomy Journal, 92, 847-854, 2000.
622 Law, B.E., Falge, E., Gu, L., Baldocchi, D. D., Bakwin, P., Berbigier, P., Davis, K., Dolman, A. J.,

623 Falk, M., Fuentes, J. D., Goldstein, A., Granier, A., Grelle, A., Hollinger, D., Janssens, I. A., Jarvis, P.,
624 Jensen, N. O., Katul, G., Mahli, Y., Matteucci, G., Meyers, T., Monson, R., Munger, W., Oechel, W.,
625 Olson, R., Pilegaard, K., Paw, K. T., Thorgeirsson, H., Valentini, R., Verma, S., Vesala, T., Wilson, K.,
626 Wofsy, S.: Environmental controls over carbon dioxide and water vapor exchange of terrestrial
627 vegetation. Agricultural and Forest Meteorology, 113, 97-120, 2002.
628 Lei, H. M., Cai, J. F., Yang, D. W. and Wang, F. J.: Long-term variability of evapotranspiration in a
629 large irrigated area in lower reach of Yellow River, Advances in Science and Technology of Water
630 Resources, 32, 13-17, 2012.
631 Lei, H. M. and Yang D. W.: Inter-annual and seasonal variability in evapotranspiration and energy
632 partitioning over an irrigated cropland in the North China Plain, Agricultural and forest meteorology,
633 150, 581-589, 2010.
634 Lei, H. M.. Ecohydrological processes in a large irrigated area of the North China plain: field
635 observation and modeling. Beijing, Tsinghua University, 2011 (in Chinese)
636 Lei, Z. D., Yang, S. X. and Xie, S. C.: Soil water dynamics, Tsing-Hua University Press, Beijing, 1988
637 (in Chinese)
638 Lettermaier, D. P. and Famiglietti, J. S.. Water from on high. Nature, 2006, 444, 562-563.
639 Li, Z., Liu, W. Z., Zhang, X. C. and Zheng, F. L.: Impacts of land use change and climate variability on
640 hydrology in an agricultural catchment on the Loess Plateau of China, Journal of hydrology, 377, 35-42,
641 2009.
642 Liang, L., Lu, S. H. and Shang, L. Y.: Numerical simulation of effect of Loess Plateau vegetation
643 change on local climate, Plateau Meteorol, 27, 293-300, 2008.
644 Liu, H. Z., Dong, W. J., Fu, C. B. and Shi, L. Q.: The long-term field experiment on aridification and
645 the ordered human activity in semi-arid area at Tongyu, Northeast China, Climatic and Environmental

646 Research, 9,378-389, 2004 (in Chinese)

647 Liu, J., He, X., Bao, H. L. and Zhou C. J.. Distribution of fine roots of salix psammophila and its

648 relationship with soil moisture in Mu Us Sand land. Journal of Desert Research, 30, 1362-1366, 2010.

649 Loukas, A., Vasiliades, L., Domenikiotis, C. and Dalezios, N. R.: Basin-wide actual evapotranspiration

650 estimation using NOAA/AVHRR satellite data, Physics and Chemistry of the Earth, 30, 69-79, 2005.

651 Ludwig, J.A., Wilcox, B. P., Breshears, D. D., Tongway, D. J. and Imeson, A. C.: Vegetation patches

652 and runoff-erosion as interacting ecohydrological processes in semiarid landscapes, Ecology, 86,

653 288-297, 2005.

654 Lunetta, R.S., Knight, J. F., Ediriwickrema, J., Lyon, J. G., Worthy, L. D.: Land-cover change

655 detection using multi-temporal MODIS NDVI data, Remote sensing of environment, 105, 142-154,

656 2006.

657 Ma, Z. G. and Fu, C. B.: Some evidence of drying trend over northern China from 1951 to 2004,

658 Chinese Science Bulletin, 51, 2913-2925, 2006.

659 Maidment, D. R.: Handbook of hydrology, 1992.

660 Mo, X. G., Liu, S. X., Lin, Z. H. and Chen, D.: Simulating the water balance of the wuding river basin

661 in the Loess Plateau with a distributed eco-hydrological model, Acta Geographica Sinica, 59, 341-347,

662 2004 (in Chinese)

663 Mahfouf, J., Ciret, C., Ducharne, A., Irannejad, P., Noilhan, J., Shao, Y., Thornton, P., Xue, Y., Yang,

664 Z. L.: Analysis of transpiration results from the RICE and PILPS workshop, Global and Planetary

665 change, 13, 73-88, 1996.

666 Moran, M. S., Scott, R. L., Keefer, T. O., Emmerich, W. E., Hermandez, M., Nearing, G. S., Paige, G.

667 B., Cosh, M. H. and Oneill, P. E.: Partitioning evapotranspiration in semiarid grassland and shrubland

668 ecosystems using time series of soil surface temperature, Agricultural and forest meteorology, 149,
669 59-72, 2009.
670 Mu, Q., Heinsch, F.A., Maosheng Zhao, M. S.,Running, S.W.: Development of a global
671 evapotranspiration algorithm based on MODIS and global meteorology data. Remote Sensing of
672 Environment, 111, 519-536, 2007.
673 Piao, S. L. and Fang, J. Y.: Seasonal changes in vegetation activity in response to climate changes in
674 China between 1982 and 1999, Acta Geographica Sinica, 58: 119-125, 2003 (in Chinese)
675 Papale, D., Reichstein, M., Aubinet, M., Canfora, E., Bernhofer, C., Kutsch, W., Longdoz, B., Rambal,
676 S., Valentini, R.,Vesala, T. and Yakir, D.: Towards a standardized processing of Net Ecosystem
677 Exchange measured with eddy covariance technique: algorithms and uncertainty estimation, 2006.
678 Penman, H. L.. National evaporation from open water, bare soil and grass. Proc. R. Soc. London, A193,
679 120-145, 1948.
680 Penman, H. L.. Vegetation and hydrology, Tech. Comm. 53, Commenwealth Bureau of Soils,
681 Harpenden, England, 1963.
682 Running, S. W. and Nemani, R. R.: Relating seasonal patterns of the AVHRR vegetation index to
683 simulated photosynthesis and transpiration of forests in different climates. Remote Sensing of
684 Environment, 24, 347-367, 1988.
685 Scott, R. L., Huxman, T. E., Cable, W. L. and Emmerich, W. E.: Partitioning of evapotranspiration and
686 its relation to carbon dioxide exchange in a Chihuahuan Desert shrubland. Hydrological Processes, 20,
687 3227-3243, 2006.
688 Shi, H. and Shao, M. A. Soil and water loss from the Loess Plateau in China, Journal of Arid
689 Environments, 45, 9-20, 2000.

690 Wang, L., Wang, Q. J., Wei, S. P., Shao, M. A. and Yi, L.: Soil desiccation for Loess soils on natural
691 and regrown areas, Forest Ecology and Management, 255, 2467-2477, 2008.
692 Wang, L., Wang Z., Liu, L.Y. and Hasi, E.: Field investigation on *salix psammophila* plant
693 morphology and airflow structure, Front. For. China, 2, 136-141, 2006.
694 Wang, Y. Q., Shao, M. A., Zhu, Y. J. and Liu, Z. P.: Impacts of land use and plant characteristics on
695 dried soil layers in different climatic regions on the Loess Plateau of China, Agricultural and Forest
696 Meteorology, 151, 437-448, 2011.
697 Wei, Z. F., Wang, D. G., Zhang, C., Liu, X. F. and Zhang, H.. Response of vegetation cover to climate
698 change and human activities in Northwest China during 1999-2010. Journal of Desert Research, 34,
699 1665-1670, 2014 (in Chinese)
700 Wilson, K., Goldstein, A., Falge, E., Aubinet, M., Baldocchi, D., Berbigier, P., Bernhofer, C.,
701 Ceulemans, R., Dolman, H., Field, C., Grelle, A., Ibrom, A., Law, B. E., Kowalski, A., Meyers, T.,
702 Moncrieff, J.,Monson, R., Oechel, W., Tenhunen, J., Valentini, R. and Verma, S.: Energy balance
703 closure at FLUXNET sites, Agricultural and Forest Meteorology, 113, 223-243, 2002.
704 Xiao, C.W., Zhou, G. S., Zhang, X. S., Zhao, J. Z. and Wu, G.: Responses of dominant desert species
705 Artemisia ordosica and Salix psammophila to water stress, Photosynthetica, 43, 467-471, 2005.
706 Xin, Z. B., Xu, J. X. and Zheng, W.: Spatiotemporal variations of vegetation cover on the Chinese
707 Loess Plateau (1981-2006): Impacts of climate changes and human activities, Science in China Series
708 D: Earth Sciences, 51, 67-78, 2008.
709 Xu, X. L., Ma, K. M., Fu, B. J., Song, C. J. and Liu, W.: Influence of three plant species with different
710 morphologies on water runoff and soil loss in a dry-warm river valley, SW China, Forest ecology and
711 management, 256, 656-663, 2008.

712 Yang, F. L. and Zhou G. S.. Characteristics and modeling of evapotranspiration over a temperate desert
713 steppe in Inner Mongolia, China. Journal of Hydrology, 396, 139-147, 2010.
714 Yang, F.. A study of the vadose zone water movement's law under the influence of vegetation—a case
715 of the Mu Us Sand land. Chang'an University, Xi'an, China, 2012.
716 Yang, L., Wei, W., Chen, L. D., Chen, W. L. and Wang, J. L.: Response of temporal variation of soil
717 moisture to vegetation restoration in semi-arid Loess Plateau, China. Catena, 115, 123-133, 2014.
718 Zhang, Y., Munkhtsetesg, E., Kadota, T. and Ohata, T.: An observational study of ecohydrology of a
719 sparse grassland at the edge of the Eurasian cryosphere in Mongolia, Journal of Geophysical Research:
720 Atmospheres (1984-2012), 110, doi:10.1029/2004JD005474, 2005.
721 Zhou, Z. X., Sun, H. and LI, Z. P.: Study on Mechanism of Water-eroded Desertification and Its
722 Control in the Loess Plateau, Arid Zone Research, 1, 29-34, 2005 (in Chinese)
723

724 **Figure and table captions**

725 Fig. 1. Location of the Loess Plateau and the map of study site (LP: the Loess Plateau;
726 black triangle: flux tower; white triangle: Yulin meteorological station; ①: Tu River;
727 ②: Yuxi River; ③: Yellow River).
728

729 Fig. 2. Land use conditions of the study site over the Loess Plateau: (a) the area that
730 has not encountered land use change (photo was taken at 11 September 2014); (b) the
731 area that has not encountered land use change and the area that has encountered land
732 use change (photo was taken at 4 July 2014).
733

734 Fig. 3. Diagram of wind rose and footprint (a) wind rose of study site by using

half-hourly wind speed and wind direction data; (b) simulated footprint by ellipse (the black line of Fig.3b is the simulated footprint; the long axis is 1682m, and the short axis is 1263m; the background is the MODIS Surface Reflectance (250 m × 250 m) on 3 January 2011. Square white dots were measured points on 25 October 2013, and the white line is the maximum boundary of bare soil area)

Fig. 4. (a) Monthly mean temperature (T_a) at the experimental site of each year and climatological normal (1954－2012 climatological normal in Yulin meteorological station); (b) monthly mean relative humidity (R_H) at the experimental site and climatological normal; (c) monthly total sunshine duration (D_S) at the experimental site and climatological normal; (d) monthly total precipitation (P) at the experimental site and climatological normal.

Fig. 5. The curves of daily NDVI in (a) zone A and (b) zone B from 1 July 2011 to 30 June 2014 in the source area.

Fig. 6. The measure of land use change (D_{lu}) of July, August and September in each period.

Fig. 7. Seasonal characteristics of daily mean evapotranspiration (ET, mm; ET _7 is the 7-days moving average values of ET), potential evapotranspiration (E_{TP}, mm; E_{TP}_7 is the 7-days moving average values of E_{TP}), weight-averaged NDVI ($NDVI_w$), and soil water stress (f_s) of surface (f_{ss}) and root zone (f_{sr}) during 1 July 2011－30

758 June 2014.

759

760 Fig. 8. The correlations between daily mean evapotranspiration (ET, mm) and its
761 controlling factors: (a) daily mean potential evapotranspiration (E_{TP}, mm); (b) daily
762 weight- averaged NDVI ($NDVI_w$); (c) daily mean soil water stress of surface (f_{ss}) and
763 (d) daily mean soil water stress of root zone (f_{sr}) in 2011—2012 excluding the data in
764 rainy days and in frozen period. (r: Pearson's correlation significance; T: T-test
765 significance; P: Partial Correlation analysis)

766

767 Fig. 9. Linear regressions between vegetation phenological change ($NDVI_w$) and
768 normalized ET ($f_{vr} = ET/(E_{TP} \times f_{sr})$, $f_{vs} = ET/(E_{TP} \times f_{ss})$) in 2011—2012 by
769 excluding the data in rainy days and frozen days.

770

771 Fig. 10. Quantitative analysis between D_{lu} and normalized ET ($f_{vr} = ET/(E_{TP} \times f_{sr})$,
772 $f_{vs} = ET/(E_{TP} \times f_{ss})$) in July—September of each period.

773

774 Table 1. Typical values of total evapotranspiration (ET), total potential
775 evapotranspiration (E_{TP}), measure of land use change (D_{lu}), and soil water stress of
776 surface (f_{ss}) and root zone (f_{sr}) in each period and in growing season of each period.

777

Table 1

	Periods	ET (mm)	E_{TP} (mm)	D_{lu} (%)	f_{ss} (dimensionless)	f_{sr} (dimensionless)
Annual (7.1-6.30)	2011-2012	375	1564	-0.5%	0.49	0.45
	2012-2013	417	1941	3%	0.50	0.46
	2013-2014	478	1912	6%	0.47	0.45
Growing season (5.1-9.30)	2011-2012	260	945	-0.7%	0.65	0.61
	2012-2013	275	1092	4%	0.67	0.63
	2013-2014	321	983	8%	0.63	0.61

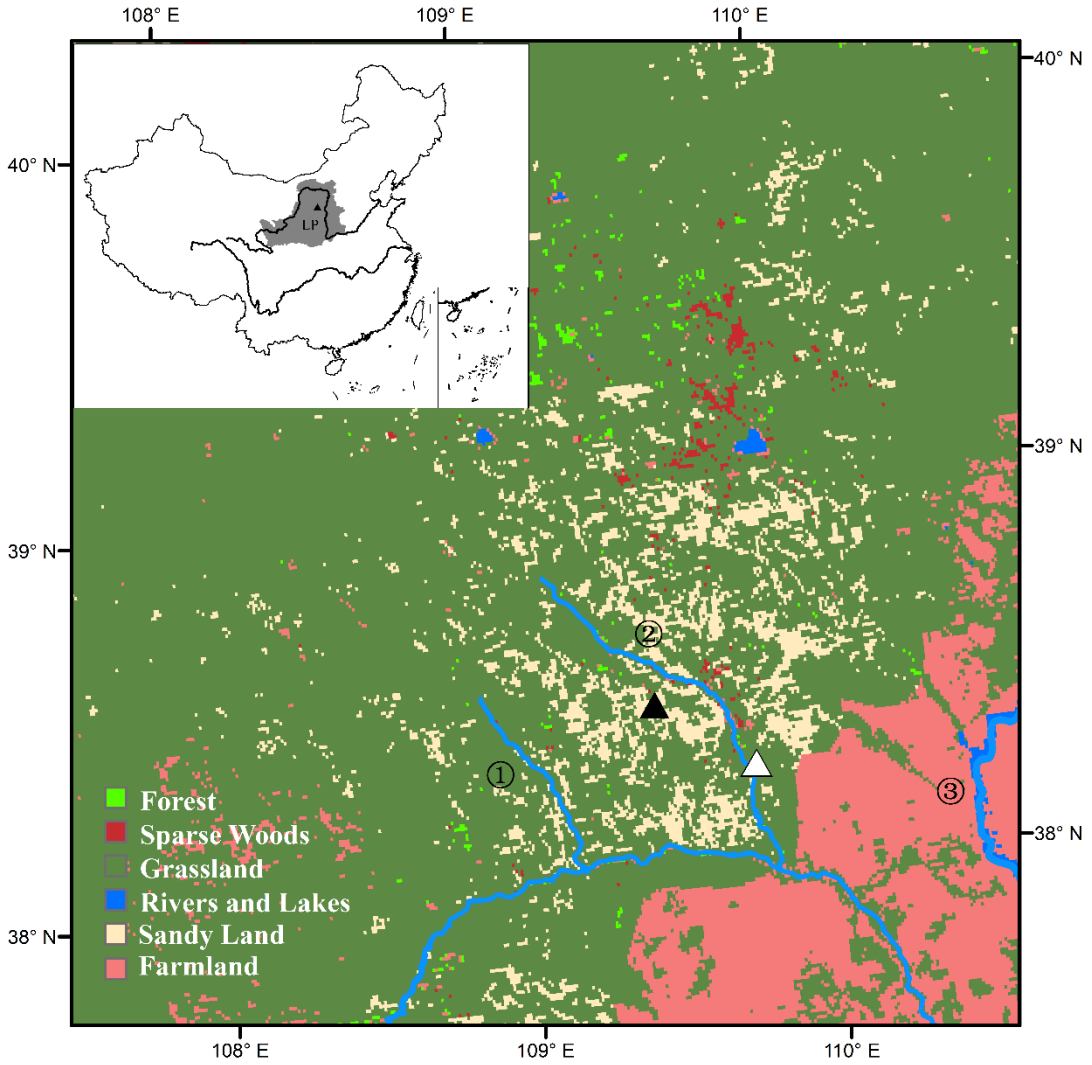
108° E
109° E
110° E
40° N
39° N
38° N
LP
①
②
③
Forest
Sparse Woods
Grassland
Rivers and Lakes
Sandy Land
Farmland

Fig. 1

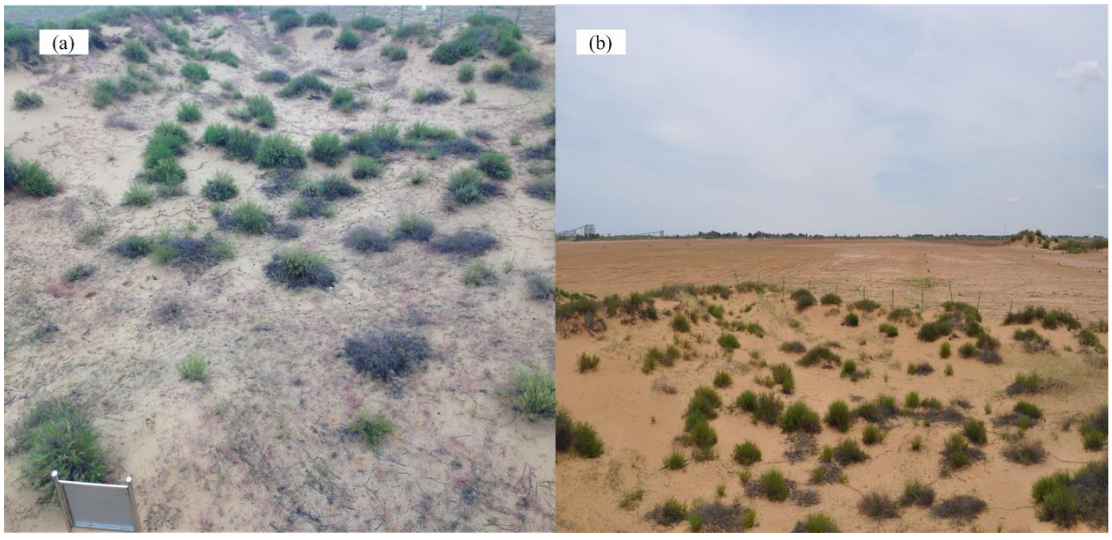
(a)
(b)

Fig.2

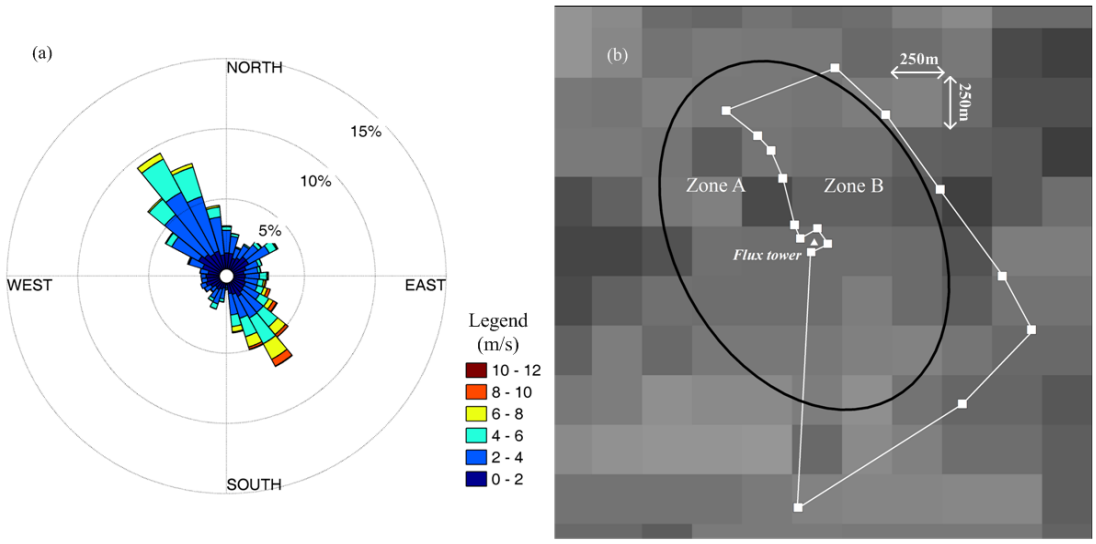
(a)
NORTH
15%
10%
5%
WEST
EAST
SOUTH
Legend
(m/s)
10 - 12
8 - 10
6 - 8
4 - 6
2 - 4
0 - 2
(b)
250m
250m
Zone A
Zone B
Flux tower

Fig.3

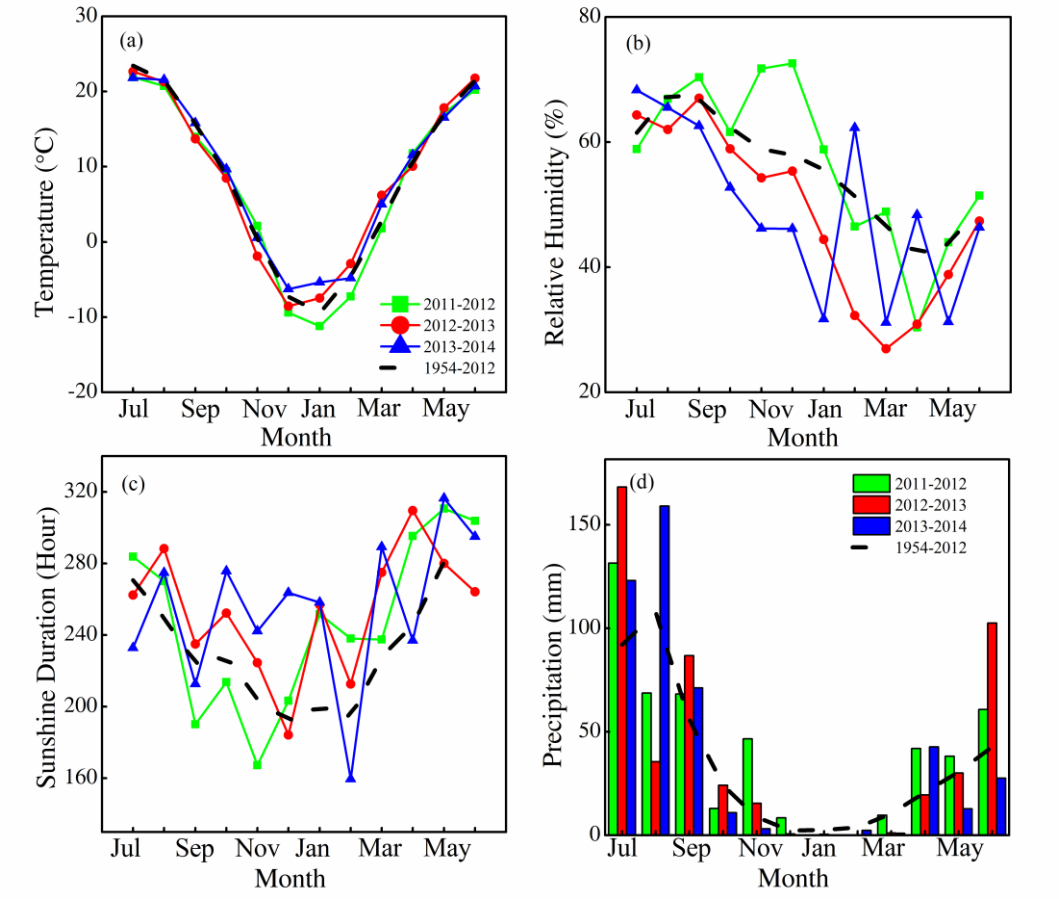
(a)
Temperature (°C)
2011-2012
2012-2013
2013-2014
1954-2012
Jul Sep Nov Jan Mar May
Month
(b)
Relative Humidity (%)
Jul Sep Nov Jan Mar May
Month
(c)
Sunshine Duration (Hour)
Jul Sep Nov Jan Mar May
Month
(d)
Precipitation (mm)
2011-2012
2012-2013
2013-2014
1954-2012
Jul Sep Nov Jan Mar May
Month

Fig.4

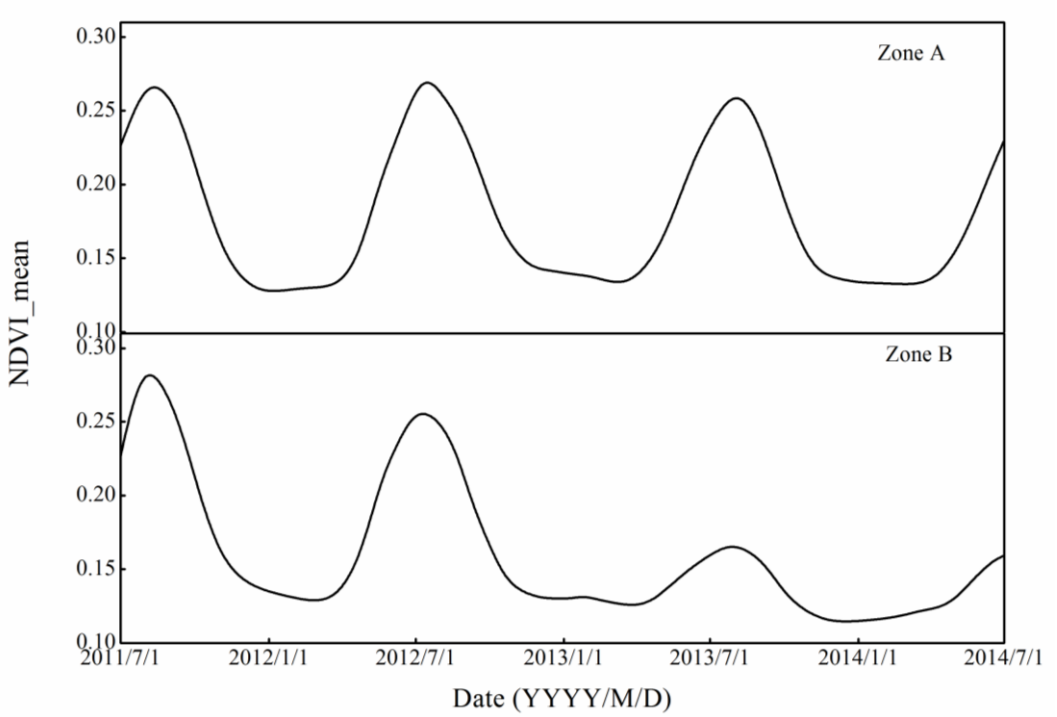
Zone A
Zone B
NDVI_mean
0.30
0.25
0.20
0.15
0.10
2011/7/1
2012/1/1
2012/7/1
2013/1/1
2013/7/1
2014/1/1
2014/7/1
Date (YYYY/M/D)

Fig.5

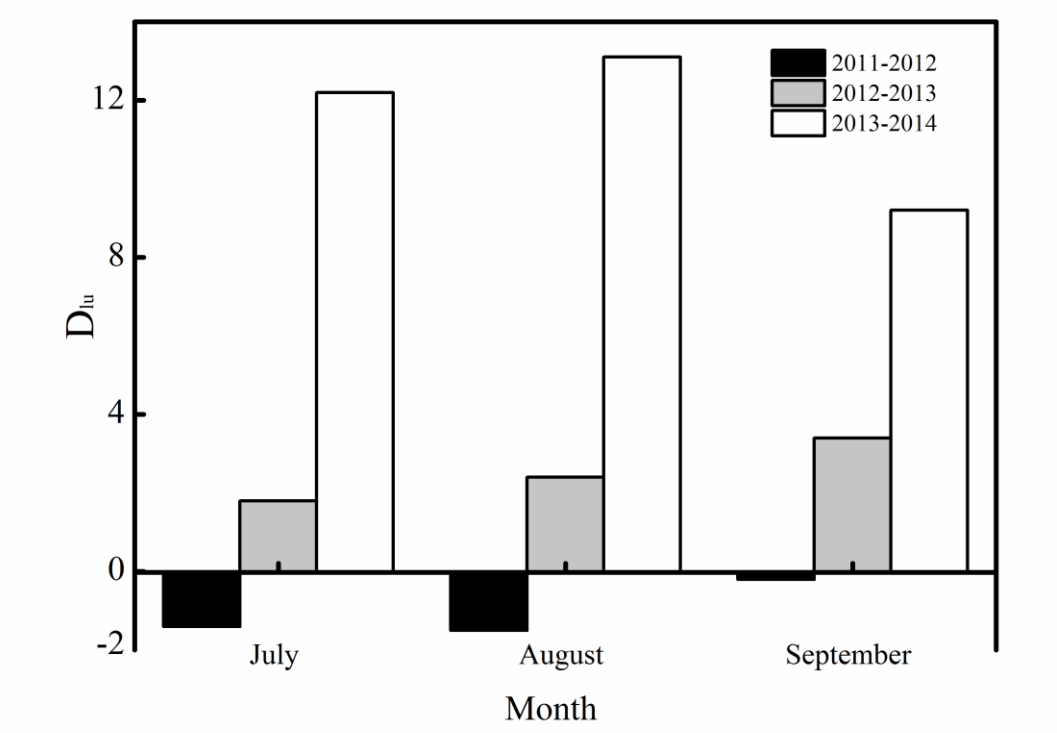
2011-2012
2012-2013
2013-2014
12
8
4
0
-2
D_{lu}
July
August
September
Month

Fig.6

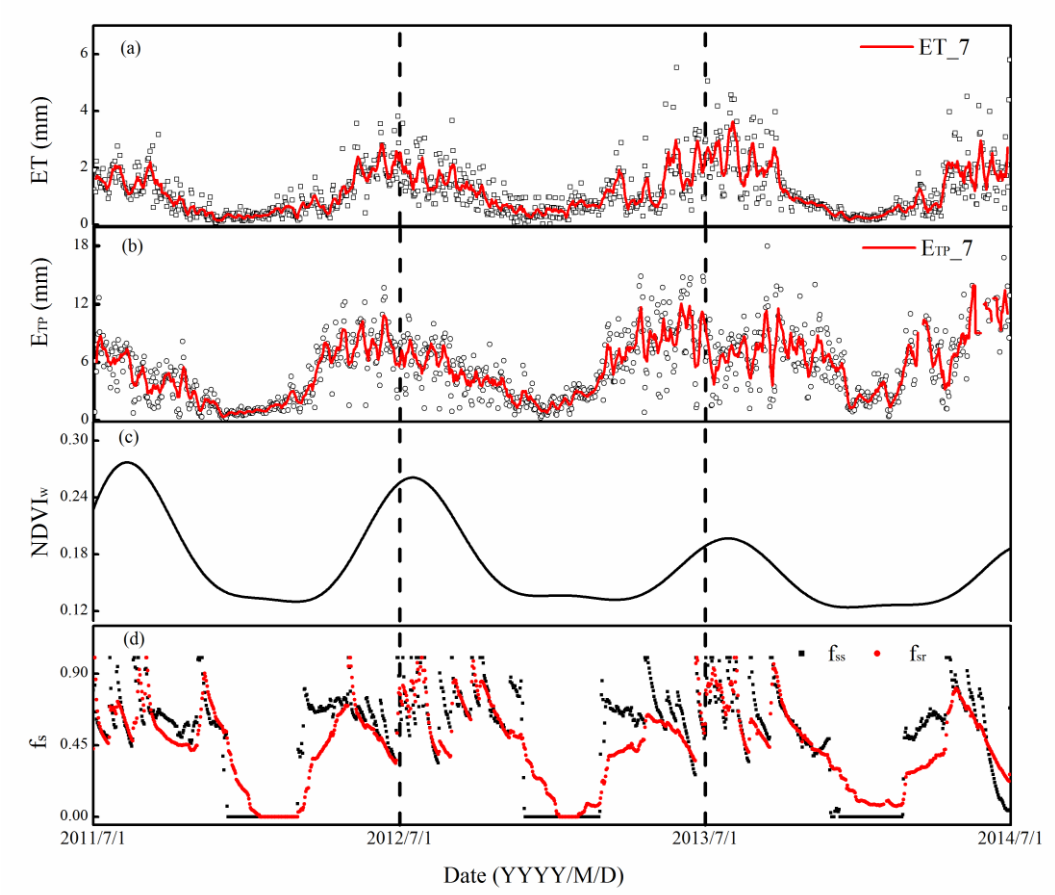
(a)
ET_7
ET (mm)
(b)
ETP_7
ETP (mm)
(c)
NDVIw
(d)
fss
fsr
fs
2011/7/1
2012/7/1
2013/7/1
2014/7/1
Date (YYYY/M/D)

Fig.7

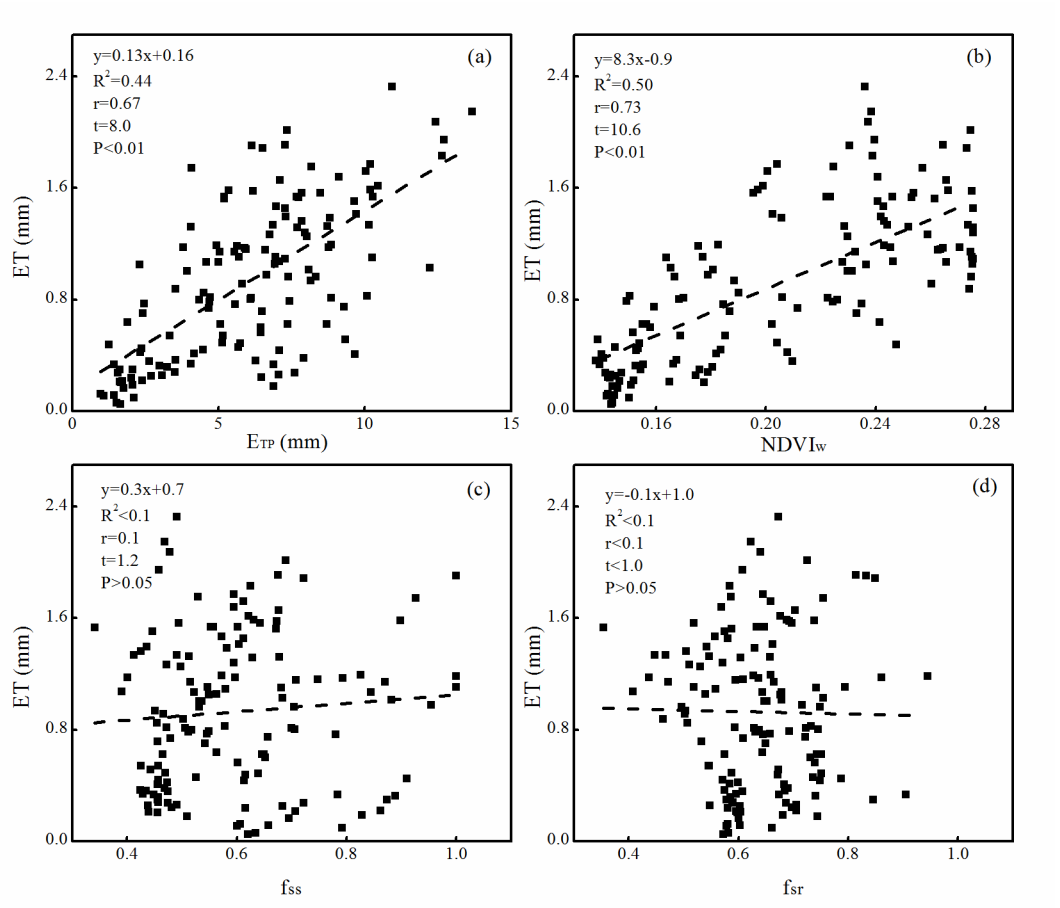
y=0.13x+0.16
R²=0.44
r=0.67
t=8.0
P<0.01
(a)
ET (mm)
ETP (mm)
y=8.3x-0.9
R²=0.50
r=0.73
t=10.6
P<0.01
(b)
NDVIw
y=0.3x+0.7
R²<0.1
r=0.1
t=1.2
P>0.05
(c)
fss
y=-0.1x+1.0
R²<0.1
r<0.1
t<1.0
P>0.05
(d)
fsr

Fig.8

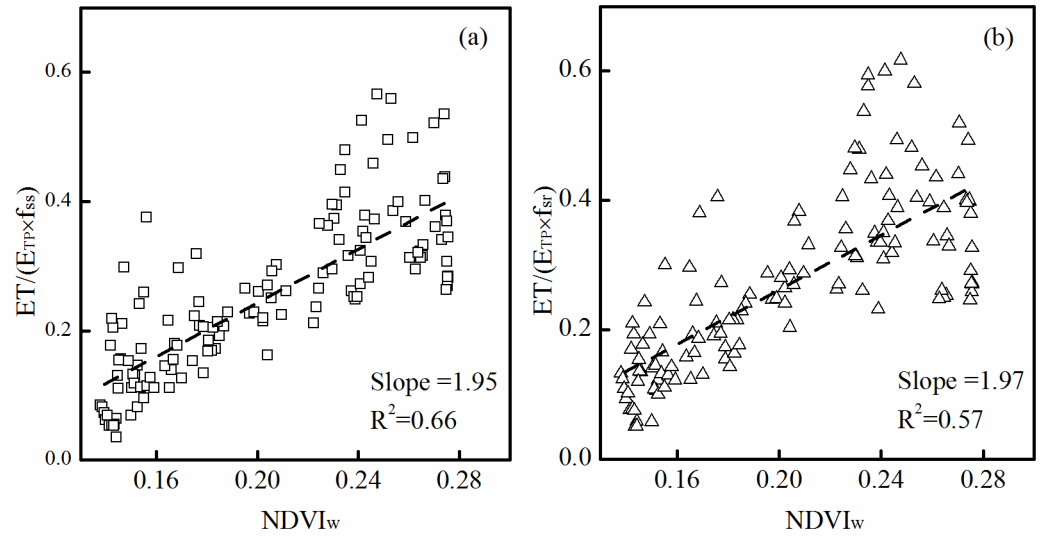
(a)
ET/(ETP×fss)
Slope =1.95
R²=0.66
NDVIw
(b)
ET/(ETP×fsr)
Slope =1.97
R²=0.57
NDVIw

Fig.9

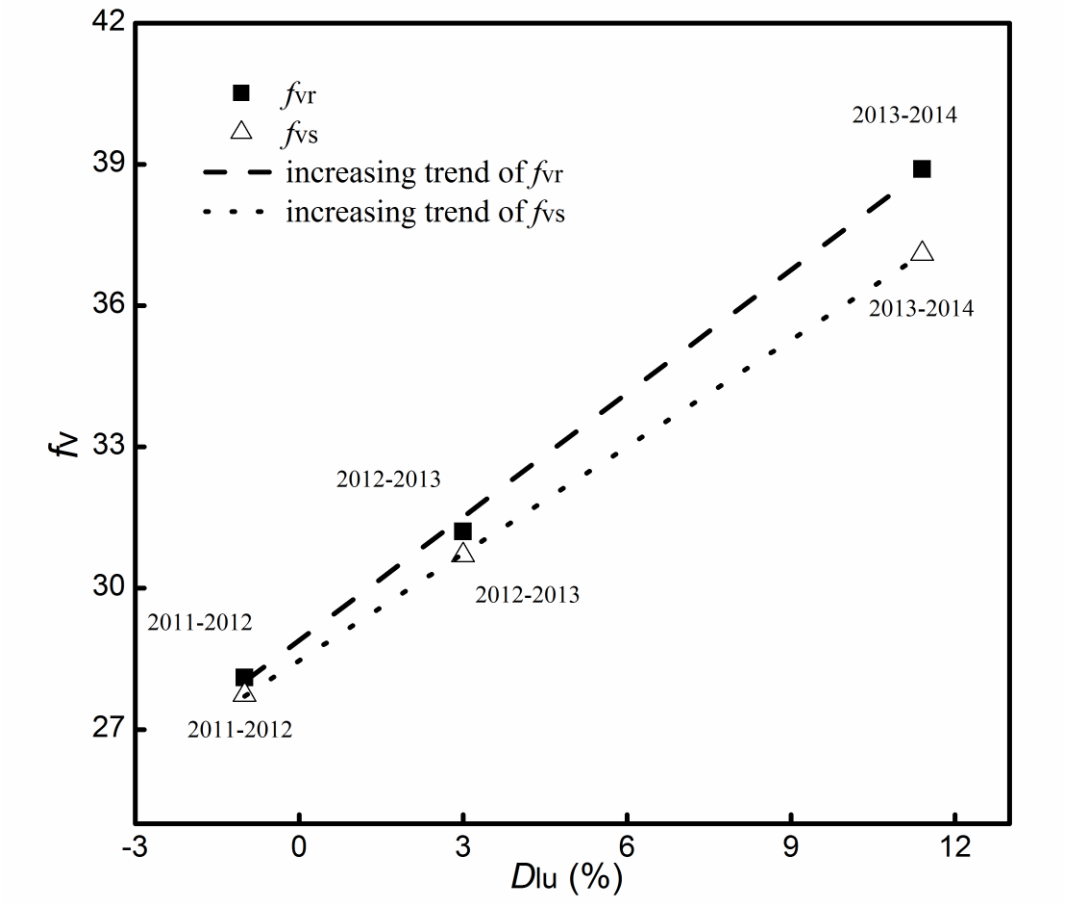
42
39
36
33
30
27
fv
-3
0
3
6
9
12
Dlu (%)
fvr
fvs
increasing trend of fvr
increasing trend of fvs
2011-2012
2012-2013
2013-2014
2011-2012
2012-2013
2013-2014

Fig.10